Variability of aerosol size-resolved composition at an Indian coastal site during the Indian Ocean Experiment (INDOEX) intensive field phase

S. Alfaro, A. Gaudichet, J.L. Rajot, L. Gomes, M. Maillé, H. Cachier

Variability of aerosol size-resolved composition at an Indian coastal site during the Indian Ocean Experiment (INDOEX) intensive field phase

S. C. Alfaro, A. Gaudichet, J. L. Rajot, L. Gomes, and M. Maillé

Laboratoire Interuniversitaire des Systèmes Atmosphériques, CNRS, Université Paris VII/Paris XII, Créteil, France

H. Cachier

Laboratoire des Sciences du Climat et de l'Environnement, Commissariat à l'Energie Atomique-CNRS, Gif-sur-Yvette, France

Received 12 June 2002; revised 8 August 2002; accepted 6 January 2003; published 17 April 2003.

[1] In March 1999, that is to say, during the Indian Ocean Experiment (INDOEX) Intensive Field Phase, various aerosol characteristics have been measured on the campus of Goa University (Goa, India: 15° 24′N, 74° 48′E). This site, located on the western coast of India, is at the exit of the continent during the winter northeastern monsoon, and the variability of the aerosol characteristics measured here will certainly reflect the variability of aerosol properties over large INDOEX areas. Concentrations in total suspended matter (TPM) and fine particles (PM1) were determined by means of a two-stage sampler. They varied greatly during the measurement period (e.g., between 30 and 120 $\mu g/m^3$ for the TPM) but were found to be, on the whole, of the same order of magnitude as those measured far downwind of the Indian subcontinent, namely at Kaashidhoo Climate Observatory (KCO, the Maldives). The aerosol mass composition determined by combining XRF analysis (for inorganic elements) and thermal analysis (for carbonaceous components) of filter samples shows that mineral dust (MD) and sea salt (SS) dominate this mass composition. For instance, temporary inputs of MD from distant desert sources explain the observed TPM variations. In contrast, aerosol number concentrations and size resolved composition determined by using optical particle counters, microscope observation, and low- or high-pressure stage impactors, reveal that in terms of numbers, black carbon (BC) is by far the dominant species in the submicron mode. These particles are frequently coated by less absorbing matter, presumably a mixture of sulfate and condensed organic compounds. By using the time variability of the K/BC ratio, it is also shown that the origin of carbonaceous components varies during the measurement period. In early March, 70% of BC is produced by fossil fuel combustion and 30% by biomass burning, but the contribution of biomass burning increases during the period of the experiment until the previous proportions are reversed around March 25. Comparison of these results with other INDOEX measurements indicates that the spatial gradient observed for aerosol concentrations and composition in the northern part of the Indian Ocean are of the same order of magnitude as the temporal variability observed at Goa. *INDEX TERMS:* 0305 Atmospheric Composition and Structure: Aerosols and particles (0345, 4801); 0365 Atmospheric Composition and Structure: Troposphere—composition and chemistry; 4801 Oceanography: Biological and Chemical: Aerosols (0305); *KEYWORDS:* INDOEX, aerosol composition, aerosol size distribution, biomass burning

Citation: Alfaro, S. C., A. Gaudichet, J. L. Rajot, L. Gomes, M. Maillé, and H. Cachier, Variability of aerosol size-resolved composition at an Indian coastal site during the Indian Ocean Experiment (INDOEX) intensive field phase, *J. Geophys. Res.*, *108*(D8), 4235, doi:10.1029/2002JD002645, 2003.

1. Introduction

[2] By scattering and/or absorbing both solar and Earth radiation, aerosols can have a significant effect on climate. Their optical properties that condition their impact on atmospheric radiative transfer mainly depend (through their complex refractive index) on their composition, state of mixing, size distribution, and shape. Due to the temporal and spatial variability of their sources and to the relative shortness of their residence time, especially in the lower troposphere, these properties are highly inhomogeneous. Computing aerosols radiative forcing in a given region thus requires accurate aerosol models. Developing such models from field measurements is particularly crucial for areas where the atmospheric aerosol load is known to be important. This is the case of the

0148-0227/03/2002JD002645

Indian Ocean over which an international campaign (Indian Ocean Experiment: INDOEX) has been designed [*Ramanathan et al.*, 1995] to study the transport towards the Arabian Sea and Indian Ocean of polluted air masses under the influence of the winter (northeasterly) monsoon.

[3] During the 1996 and 1998 INDOEX pre-campaigns or during the 1999 Intensive Field Phase (IFP) an international fleet of instrumented ships and planes has been used to investigate punctually the aerosol composition and optical properties over the Indian Ocean [*Ramanathan et al.*, 2001]. These properties have also been measured continuously at the Kaashidhoo Climate Observatory (KCO) in the Republic of the Maldives [*Satheesh et al.*, 1999; *Lelieveld et al.*, 2001], located far downwind of the Indian subcontinent. The aim of this paper is to document the aerosol phase before its transport over the ocean by results of measurements performed on the campus of the Goa University (Goa, India: 15° 24′N, 74° 48′E) during the 1999 INDOEX IFP. In the first part of this paper instruments and methods are presented. The second part focuses on aerosol size distributions and composition retrieved from ground-level measurements. Reasons explaining the variation with time of major aerosol components are analyzed but, afterwards, special attention is paid to submicron particles because of their importance in terms of optical properties in the visible spectrum. In particular, the contribution of biomass burning to the atmospheric load in carbonaceous components is assessed. Finally, results obtained at Goa are compared to results of measurements performed over the North Indian Ocean (NIO), but further away from the coast, during the 1996 and 1998 INDOEX pre-campaign cruises or during the 1999 IFP.

2. Experiment

2.1. Site Location

[4] The Goa University campus is located on the western coast of India (Figure 1), about 500 km south of Mumbaï (Bombay) and 5 km south of the Goa State capital city (Panjim, pop: 70,000). The experimental site is bounded by the Arabian Sea on its western side, by a large estuary on its southern side and by land on the other sides. The instruments were implemented about 10 m above the ground on the terrace of a small isolated building. This building was surrounded by a very sparsely vegetated lateritic cuirasse rich in Fe and Al as indicated by its reddish-brown color. Though not exclusively, experiments on the Goa site were essentially carried out between March 1 and March 26, 1999. The instruments used during this period may be separated into two categories: those aiming at determining the aerosol composition at ground level and those measuring ground level or vertically integrated optical properties. The primary objective of this paper being the determination of aerosol characteristics at ground level, instruments belonging to the first category only are presented here. Those belonging to the second one are described in a paper (S. C. Alfaro et al., manuscript in preparation, 2003) focusing on the aerosol optical properties.

2.2. Material and Methods

2.2.1. Aerosol Mass Concentrations and Size Distribution

[5] For assessing the time dependence of aerosol mass concentrations, aerosol samples were collected between March 2 and March 26, 1999 on pre-weighted nuclepore filters with a 2 stage aerosol sampler. This sampler known as the "Gent stacked filter unit (SFU) has been described by *Hopke et al.* [1997]. Sampling was performed at ambient humidity (recorded every 5 minutes with a Vaisala probe, model HMP 35AC), and collection duration extended from about 6 to 12 h. At the flow-rate used in the experiment (1.1 m^3/h) the cut-off aerodynamic diameter between the two stages of this sampler is approximately 1 μm. Thus the average mass concentrations in particles smaller than 1 μm (PM1), in 'coarse' particles larger than 1 μm (CM), and in 'total particle matter' (TPM = PM1 + CM) could be derived simply for each sampling period by weighting both filters after drying.

Figure 1. Map showing the location of the Goa University experimental site and of the Kaashidhoo Climate Observatory (KCO, the Maldives).

[6] During the experiment several instruments listed in Table 1 were also run in parallel to determine more precisely the aerosol size distribution at ambient humidity. Between March 20 to March 26 particle number concentrations were measured continuously in 6 diameter classes (0.3–0.5, 0.5–0.7, 0.7–1.0, 1.0–2.0, 2.0–5.0, >5.0 μm) by the means of an optical size analyzer (OSA, model MET ONE 237B). According to the manufacturer, the precision of the measurements is better than 5% in each size class.

[7] A condensation particle counter (CPC, model TSI 3022A) coupled to a diffusion battery (DB, model TSI 3040) was operated manually at 25 different times between March 13 and March 23. The CPC provided the total concentration of particle having a diameter between 0.007 and 3 μm (with a 100% efficiency above 0.02 μm), while the DB provided the parameters (mean geometric diameter, geometric standard deviation and amplitude) of the best lognormal fit to the size distribution of particles having a diameter between 0.02 and 0.2 μm. When the OSA and CPC counters were run in parallel (13 occurrences between March 20 and March 26), subtracting the number of particles larger than 0.3 μm (as measured by the OSA) to

Table 1. List of the Instruments Used for Chemical or Physical Characterization of the Aerosol at Goa During the INDOEX Intensive Field Phase (See Text for Details)

	Specific Working Conditions		
Type of Instrument	Filter Type	Flow Rate	Purpose or Chemical Analysis
Low-volume sampling lines (×2)			
1st line	Nuclepore 0.4 μm	1 m^3/h	TEM and SEM (+EDS), XRF
2nd line	Whatman (quartz)	-	BC, OC concentrations
Stacked filter unit			
1st stage	Nuclepore 0.8 μm	1.1 m^3/h	Coarse particle mass concentration
2nd stage	Nuclepore 0.4 μm	-	PM1 mass concentration
Cascade Impactors			
EGA	Nuclepore 0.4 μm	1 m^3/h	IC, XRF
DLPI	Nuclepore 0.4 μm	0.6 m^3/h	
CPC			Particle number concentration
OSA, Diffusion Battery			Number size distribution
Aethalometer			BC concentrations

the CPC measurements provides an additional size class (<0.3 μm) to the six ones directly available from the OSA counter. An iterative procedure based on a least square routine [*Gomes et al.*, 1990] can then be applied to determine the parameters of the 2 or 3 lognormal distributions the combination of which best fits the number of particles measured in the seven size classes mentioned above. These mathematical functions do not necessarily correspond to real particle populations, but they can prove useful in that they help simplify the representation of the overall aerosol size distribution, especially when bulk aerosol is a complicated mixture of numerous components as is the case at Goa (see below).

2.2.2. Aerosol Composition

[8] Black carbon (BC), sea-salt (SS), non-sea salt sulfates (NSS), other non-sea salt water soluble such as nitrate (WS), non absorbing condensed organic phases (particulate organic matter, POM), and mineral dust (MD) are expected to be the main aerosol components over the polluted site of Goa as well as on a large part of the northern Indian Ocean. In order to determine the apportionment of the Goa aerosol between these components, several parallel measurements have been performed.

2.2.2.1. Inorganic Components

[9] Low-volume sampling lines have been used between March 1 and March 26, 1999, to collect aerosol particles on 0.4 μm-Nuclepore filters at ambient humidity, and at a constant flow rate ($1 m^3.h^{-1}$). In these experimental conditions the omni-directional sampling inlets that were used [*Liu and Piu*, 1980] have a 20 μm estimated cut-off size. The filters were submitted to X-ray fluorescence analysis (XRF, Phillips, model PW2404) or observed under transmission (TEM, JEOL, model 100 CXII) or scanning (SEM, JEOL, model JSM 6301F) electron microscopes (see below). XRF provides the mass of major (Al, Si, Na, S), or trace (K, Fe, ...) inorganic elements collected on each filter. By using the average Al mass fraction in mineral dust that is about 8% [*Taylor*, 1964], the bulk aerosol mass concentration in mineral dust (MD) can be retrieved from Al mass concentrations:

$$MD = A1/0.08 \quad (1)$$

In a similar manner, the atmosphere concentration in sea salt (SS) can be obtained from Na concentrations once a correction (0.1Al) due to the presence of Na in mineral dust has been taken into account [*Chiapello et al.*, 1999]:

$$SS = 3(Na - 0.1\,A1) \quad (2)$$

Finally, concentration in non sea-salt, non mineral sulfates (NSS), assumed to be under the form of ammonium sulfate, can be derived from S measurements by the following equation [*Chiapello et al.*, 1999] accounting for crustal and sea-salt component sulfur:

$$NSS = 4.19(S - 0.082Na - 0.0018A1) \quad (3)$$

2.2.2.2. Carbonaceous Components

[10] An aethalometer (model AE 14, Magee Scientific) was run continuously on the site from February 16 to March 26, 1999. This instrument measures almost in real time (every 5 minutes) the variation of the absorptance of a filter on which the ambient aerosol is progressively accumulated by air filtration at 10 L/min flow rate. Assuming a constant value, to be determined experimentally, for the mass absorption efficiency (σ_{abs}) of BC considered as the only absorbing aerosol component, the instrument provides time series of the atmospheric mass concentration in equivalent BC. Results are corrected for the apparent enhancement that happened at each automated change of measurement spot on the tape.

[11] Other aerosol samples collected on precleaned Whatman quartz filters between March 1 and March 22 were submitted to decarbonation and thermal analysis according to a method described by *Cachier et al.* [1989]. This provides the ambient air mass concentration in total carbon (TC), and in its BC fraction. The precision of the method is estimated to 10%. The missing (TC-BC) organic carbon (OC) is attributed to the presence of particulate organic matter (POM). It is usually considered [*Liousse et al.*, 1996] that the POM concentration can be evaluated from that of OC by:

$$POM = 1.4\,OC \quad (4)$$

2.2.3. Size-Resolved Composition

2.2.3.1. Cascade Impactors

[12] In order to assess the size resolved composition of the aerosol, a custom made EGA 80 low-volume cascade

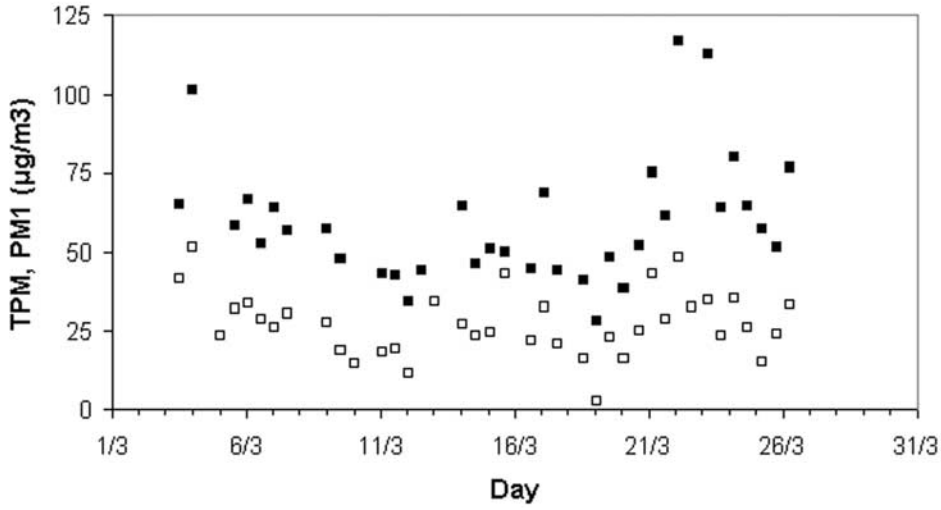

Figure 2. TPM (black squares) and PM1 (open squares) concentrations deduced from direct weighting of two stage-impactor filters (see text for details).

impactor [*Bergametti et al.*, 1982] was used from March 11 to March 23 to sort aerosol samples according to their aerodynamic sizes. At the nominal flow rate of 1 $m^3.h^{-1}$ the 50% aerodynamic cutoff diameters of the five stages of this impactor are 8.75, 3.90, 1.95, 1.25, and 0.65 μm. A final backup filter is also used as an additional stage to collect all the very fine particles that have not impacted on the first five stages. Because the cut-off diameters of the various stages are mostly in the super-micron range, this impactor is mainly used to assess the size distribution of relatively coarse species. Some of the samples collected with it have been analyzed by XRF to determine the mass of mineral dust and sea salt present on each impactor stage. Suppressed ion chromatography (IC) has been used on other samples to determine the mass of major soluble anions (Cl^-, SO_4^-, NO_3^-) present on each stage. With both analysis methods the fitting procedure already mentioned above [*Gomes et al.*, 1990] can be used to provide the mass amplitude (A_m), geometric mean diameter (d_m) and geometric standard deviation (σ_m) of the best lognormal fit to the measurements. Assuming sphericity of the particles, these mass results can be converted into number ones by using the following equations [*Seinfeld and Pandis*, 1998] in which the number parameters (subscript n) are expressed as functions of the mass ones and of the particle density, ρ_p.

$$\sigma_n = \sigma_m \tag{5}$$

$$d_n = \exp\left(\ln(d_m) - 3\ln^2\sigma_m\right) \tag{6}$$

$$A_n = A_m / \left(\pi/6\rho_p {d_m}^3\right) \tag{7}$$

A DEKATI low-pressure impactor (DLPI, DEKATI Ltd) working at a nominal flow rate of 10L/mn has also been used punctually on three occasions between March 11 and 12 before its pump broke off. This device provides a much better separation of the particles in the submicron range than the EGA impactor. Indeed, the aerodynamic cut-off diameters of its 13 stages are 0.03, 0.058, 0.103, 0.167, 0.256, 0.395, 0.640, 1.00, 1.62, 2.47, 4.00, 6.62, and 10.24 μm. It is mostly useful for determining the size distribution of inorganic elements having a strong submicron component, especially S and K (see below). These elements are particularly important because they are linked, respectively, to non sea salt sulfate (equation (3)) that is usually considered as a major aerosol component in polluted areas, and to some BC particles - those for which a high K/BC ratio is a fingerprint of their biomass burning origin. As in the case of the EGA impactor, results can be expressed in terms of mass (or number) parameters of lognormal modes after the aforementioned deconvolution procedure has been applied to the measurements.

2.2.3.2. Microscope Observations

[13] When coupled to energy dispersive spectrometry (EDS) that allows determination of particulate individual elemental composition, TEM observation of aerosol samples collected on nuclepore filters provides identification of particles belonging to different species as well as qualitative and quantitative assessment of their morphological characteristics. Number size distributions of the various particles can also be obtained by visual sizing and counting. If necessary, these size distributions can be converted into mass size distribution by using (5), (6), (7).

3. Results and Comments

3.1. Aerosol Mass Composition

3.1.1. TPM and PM1 Mass Concentrations

[14] For the measurement period the average TPM and PM1 mass concentrations are 59.9 and 27.2 μg/m3, respectively, but important fluctuations are observed around these mean values (Figure 2). From high values at the beginning of the measurement period TPM and PM1 concentrations drop to a minimum reached around March 12, this decrease is followed by a first peak for both concentrations observed

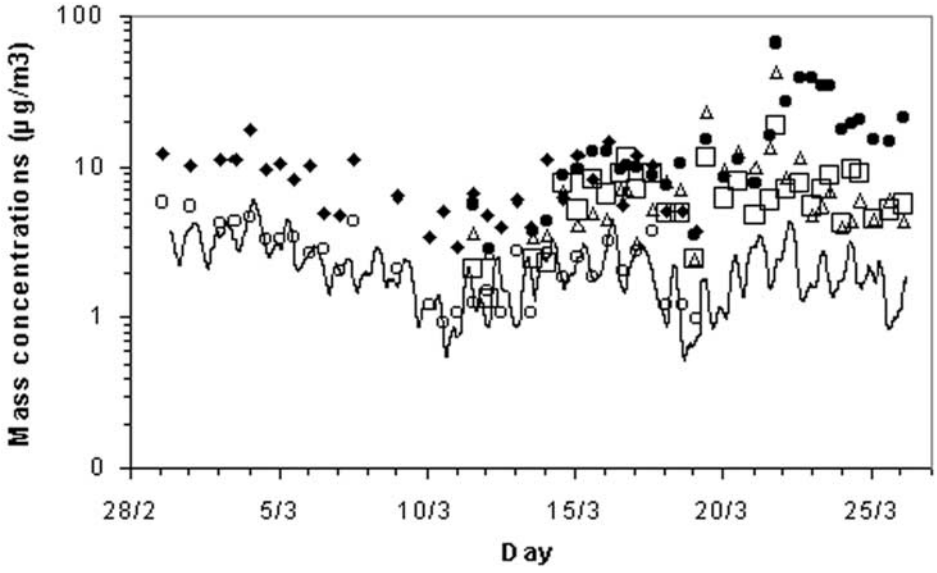

Figure 3. Bulk mass concentrations in mineral dust (solid circles), non mineral and non sea salt sulfate (open squares), and sea salt (open triangles) as determined by XRF analysis. Black carbon (open circles) and organic carbon (solid diamonds) concentrations have been determined by thermal analysis. Black carbon concentrations derived from aethalometer measurements have also been represented (continuous line).

between March 12 and March 20, then by a second one, relatively more pronounced for the TPM than for the PM1, reached around March 22–23. In the meantime, the ratio PM1/TPM computed from the previous values does not show any visible trend. Its remains between 40 and 60% except just before the end of the observation period when it drops to about 30% because of the temporary increase in TPM concentrations that, at this particular time, is not accompanied by a corresponding increase in PM1.

3.1.2. Aerosol Components

[15] Mass concentrations of SS, NSS, and MD are plotted versus time in Figure 3. Averages of 4 punctual IC measurements of sulfate, chloride, and nitrate concentrations are 3.6 (±1.6), 3.5 (±2.6), and 4.1 (±2.6) $\mu g/m^3$, respectively.

[16] Concentrations of carbonaceous species have also been added in Figure 3. BC, and OC concentrations have been determined by thermal analysis of quartz filters. For BC, concentrations derived at a very short time step (every 5 minutes) from aethalometer measurements have also been reported. The BC mass absorption efficiency required for this derivation (see above) has been chosen in order to provide the best agreement between thermal and optical methods at times when both measurements were simultaneously available. This direct calibration of the aethalometer yields σ_{abs} = 17.6 m^2/g. The high time resolution of this instrument shows the existence of a diurnal concentration cycle. A ratio of about 2 is obtained between early morning and late evening concentrations. This can be explained on the one hand by the nocturnal decrease in boundary layer height combined with topographical effects on air masses circulation [*Leon et al.*, 2001] that lead to a general increase in aerosol concentrations during the night, and on the other hand by the fact that land breeze is probably more polluted than marine air.

[17] At a larger time scale, the decrease in TPM and PM1 concentrations measured between March 1 and March 12 is also observed for carbonaceous components (BC and OC) measured during this period. When concentrations of all main species become available (after March 12) it can be seen that they vary with time, but not always in the same proportions. Indeed, based on the MD concentration behavior, the observation period can be split roughly into two subperiods: period 1 (P1) between March 12 and March 21, and period 2 (P2) after March 21. During P1, MD concentrations remain below 15 $\mu g/m^3$ (Figure 3) and represent about 30% of the measured TPM (Table 2). The corresponding dust can probably be considered as having been mobilized locally, essentially by foot or motorized traffic. During P2, MD concentrations raise dramatically to reach values as high as 40 $\mu g/m^3$. This can be explained by long-range advection of dust produced by wind erosion in Arabian deserts [*Leon et al.*, 2001]. Evidence for this difference in dust origin can be confirmed by using the Al/Fe ratio determined from XRF analysis. During P1, the low value of this ratio (1.14 ± 0.20) (Figure 4) is characteristic of the ferralitic soils encountered in the Ghâts at the latitude of Goa [*Peterschmitt*, 1993]. On the contrary, the significantly

Table 2. Average Mass Contribution of Each Aerosol Species to the TPM[a]

Period	BC	POM	NSS	SS	MD	WS
P1	5 (2)	22 (7)	13 (4)	23 (8)	29 (5)	8 (2)
P2	3 (1)	20 (8)	9 (2)	15 (7)	45 (9)	8 (1)

[a]Values are given in percent. Standard deviations are indicated between brackets. Period P1 corresponds to 'usual conditions' and P2 to a particular period when coarse dust was advected to Goa from Pakistani deserts (see text for details).

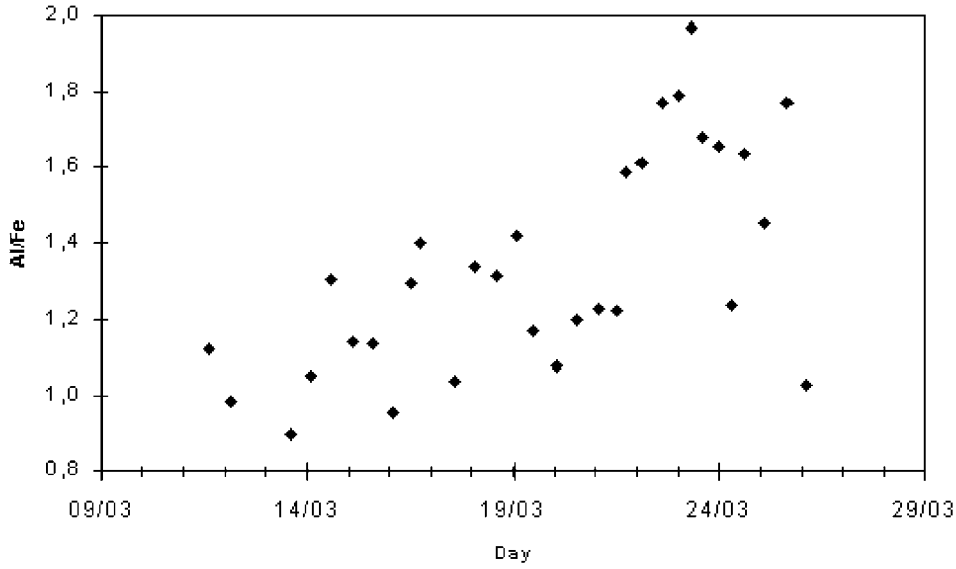

Figure 4. Al/Fe ratio determined from XRF measurements performed on nuclepore filters. The sharp increase observed between March 22 and 24 reveals that mineral dust inputs observed at Goa at this time are not of local origin (see text for details).

higher Al/Fe value (1.60 ± 0.26) observed after the March 22 sharp increase in dust concentration is typical of Arabian deserts [*Goldschmidt*, 1958]. Due to selective advection of MD, the mass proportion of this component reaches 45% of the TPM during P2 (Table 2).

[18] During both P1 and P2, MD, SS, POM, and NSS are major contributors to the aerosol mass load. Nitrate explains about 8% of the mass load. This value for nitrate is in good agreement with the 7% determined by C-130 aircraft measurements over the North Indian Ocean [*Ramanathan et al.*, 2001]. BC mass contribution is much lower. It accounts for 3 to 5 % of the TPM, that is to say 6 to 10% of PM1 if one uses the fact that BC is in the PM1 size range and the value (0.5) of the PM1/TPM ratio.

3.2. Contribution of Chemical Species to Number Size Distribution

[19] Thirteen size distributions measurements have been performed with the CPC and the OSA during a period (from March, 20 to March, 25) encompassing the end of P1 and P2. The average humidity for this period is 85 (±10) %. Deconvolution of these measurements show that the aerosol size distributions can always be reproduced by the means of only three lognormally distributed modes (Table 3). The average values of the mean geometric diameter (gmd) and of the geometric standard deviation (gsd) obtained by this method for the finest of these modes (mode 1) are in good agreement with the results provided independently by the DB measurements (also reported in Table 3). This similarity in results obtained by two physically different methods suggests that the optical counter measurements are not significantly biased by the fact that it has been calibrated with non absorbing latex spheres.

[20] The amplitudes of the finest and second finest populations (A_1 and A_2, respectively) are found to be larger in the morning than in the afternoon by a factor of about 2, which is consistent with the explanation provided above to explain BC diurnal cycle. During P1, the mean value of the ratio A_1/A_2 is 1310 ± 65 (standard deviation). This value is significantly larger than the one found during P2 (540 ± 180). During the measurement period, the amplitude of the coarsest mode (CM or mode 3) is found to be about 5 orders of magnitude lower than the one of mode 1 (Table 3), but because of the uncertainties attached to determination of this low amplitude no day/night effect can be distinguished in this case.

[21] In order to determine the physical characteristics of absorbing particles, aerosol samples collected during the second half of March were examined under the TEM and the SEM. Numerous individual spherical particles (Figure 5a) were detected. Their composition determined by EDS (Figure 5b) shows that they are essentially carbonaceous

Table 3. Characteristics of the Three Lognormal Modes Identified in the Ground-Level Aerosol at Goa: Geometric Mean Diameter, Geometric Standard Deviation, and Amplitudes of All Three Modes Obtained by Deconvolution of Optical Counter Measurements[a]

	N	Mode 1	Mode 2	Mode 3
gmd, μm				
deconv.	13	0.098 ± 0.013	0.92 ± 0.06	3.95 ± 0.065
DB	13	0.101 ± 0.012		
gsd				
deconv.	13	1.72 ± 0.13	1.69 ± 0.19	1.97 ± 0.08
DB	13	1.85 ± 0.14		
Amplitude, m^{-3}				
morning	7	$(11.1 \pm 2.5)\ 10^9$	$(18.9 \pm 1.0)\ 10^6$	$(4.06 \pm 0.07)\ 10^5$
afternoon	6	$(6.3 \pm 1.7)\ 10^9$	$(6.8 \pm 4.6)\ 10^6$	-

[a]Here, gmd, geometric mean diameter; gsd, geometric standard deviation; deconv., deconvolution. Mode 1 gmd and gsd have also been obtained by the means of a diffusion battery (see text for details). N is the number of measurements.

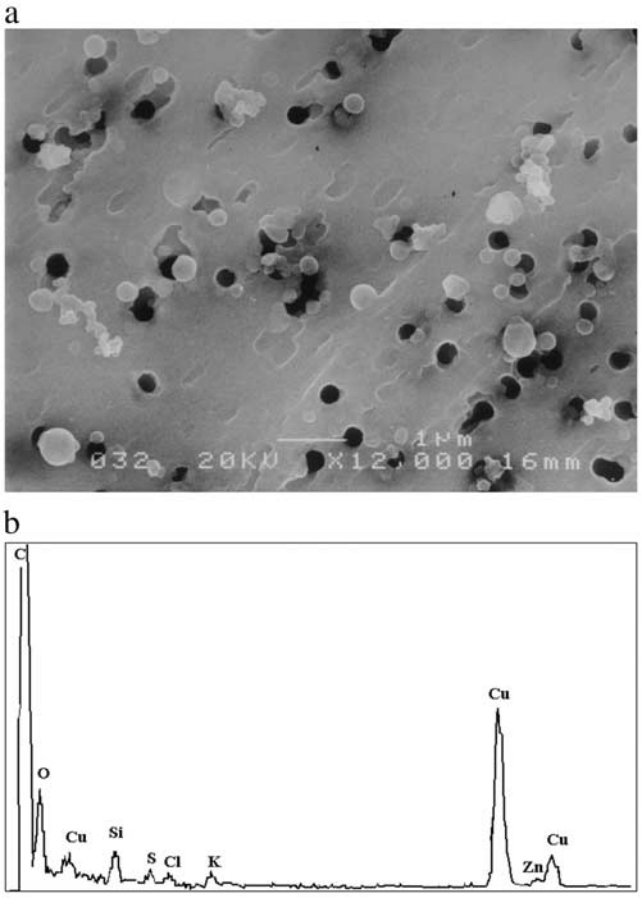

Figure 5. Scanning electron microscope observations (a) of spherical particles collected at Goa. Their composition determined by energy-dispersive spectrometry (b) shows that they are essentially made of carbon with a low-K content. These particles are characteristic of biomass burning.

particles with a low-K content. These particles are characteristic of smoldering biomass burning [*Gaudichet et al.*, 1995; *Martins et al.*, 1998]. Their average dry number diameter determined by visual sizing of about one hundred of them is found to be close to 0.4 μm, which locates them in mode 2 of the aerosol size-distribution. The corresponding BC fraction will hereinafter be noted BC2. A second type of absorbing particles can be found in a much smaller size range (less than 0.1 μm). Though these particles are frequently seen to be aggregated on the nuclepore filters (Figure 6), they must correspond to a carbonaceous component (CC1) of mode 1. Some of these particles are made of a soot core (SC) surrounded by a gelatin-like non-absorbing coating. They are similar to those observed in biomass burning plumes in Brazil [*Reid and Hobbs*, 1998; *Martins et al.*, 1998]. Their coating is likely made of a mixture of sulfate and organic compounds. This type of coating not only alters the optical properties of the soot, it may also enhance its hygroscopic properties [*Saxena et al.*, 1995]. The diameter of the dry coated particles determined by visual sizing is of about 0.08 μm, and the one of the soot cores is assumed to be the one (0.023 μm) of single soot particles [*Gaudichet et al.*, 1995; *Hess et al.*, 1998]. It has to be noted that, because POM is produced by condensation of organic compounds released at high temperature during biomass combustion, it is probable that most of POM can be found under the form of soot core coatings.

[22] It is possible to determine the order of magnitude of the unknown number fraction of CC1 in mode 1 (p_1) and of BC2 in mode 2 (p_2) by noting that the mass concentration of BC (C_{BC}) measured by the aethalometer at each time is the sum of mode 1 and 2 contents in BC (C_{BC1} and C_{BC2}, respectively), themselves depending on p_1 and p_2. If we assume that the mass density (ρ_{BC}) of the CC1 soot cores (SC) and that of BC2 particles is the same (1.9 g/cm^3 [*Seinfeld and Pandis*, 1998]), this leads to the following equation:

$$C_{BC} = \pi/6\rho_{BC}\left(p_1 A_1 d_{SC,m}{}^3 + p_2 A_2 d_{BC2,m}{}^3\right), \qquad (8)$$

where $d_{SC,m}$ and $d_{BC2,m}$ stand for SC and BC2 mass diameters. They are computed from $d_{SC,n}$ (=0.023 μm), $d_{BC2,n}$(=0.4 μm), σ_{SC}(=1.8), and σ_{BC2}(=1.7) by using (6).

[23] The p_1 and p_2 values are then determined by a least square iterative routine intended to provide the best agreement between all the measured C_{BC} values and those computed from (8). It is found that $p_1 = 0.7$ and $p_2 = 0.1$. There is an independent way of checking the dominance of BC over mode 1 indicated by the high p_1 value. Indeed, the fact that a significant fraction of BC is found in mode 1 should imply a strong correlation between the amplitude of this mode (A1) and the atmospheric content in BC as measured for example by the aethalometer. Such a correlation exists (Figure 7), and a significant ($r^2 = 0.85$ for 13 points) linear dependence of A1 to BC (in μg/m^3) is obtained:

$$A1 = 4.1\,10^9 BC \qquad (9)$$

[24] The 70% number proportion of CC1 in mode 1, and 10% of carbonaceous particles in mode 2 are also consistent with *Guazzotti et al.*'s [2001] observations. Indeed, by using time of flight mass spectrometry to analyze the composition of individual particles over the INDOEX area these authors found that at northern latitudes (Arabian Sea) as much as 80% of particles with aerodynamic diameter between 0.2 and 0.3 μm (the lowest size range they investigated) were carbonaceous, but that this proportion dropped to 20% in the 0.9/1.0 μm range and to 10% between 1.0 and 1.1 μm.

[25] The contribution of inorganic species to the aerosol number size distribution can also be assessed. Deconvolutions of XRF analysis performed on aerosol samples collected by cascade impactor essentially between March 22 and March 24 reveal the presence of a mineral dust component of fairly constant geometric mass median diameter (2.9 ± 0.2 μm) and geometric standard deviation (1.6 ± 0.2). Over the measurement period the mass amplitude is 28.3 ± 9.7 μg/m^3. By assuming a dust mass density of 2.5 g/cm^3, the characteristics of the number dust size distribution can be computed from the mass ones by using (5), (6), and (7). This leads, to $d_n = 1.5$ μm, $\sigma_n = 1.6$, and $A_n = 1.5\ 10^6 \pm 5\ 10^5$ m^{-3}. Thus, the number proportion of mineral dust particles amounted to about 10% of the amplitude of

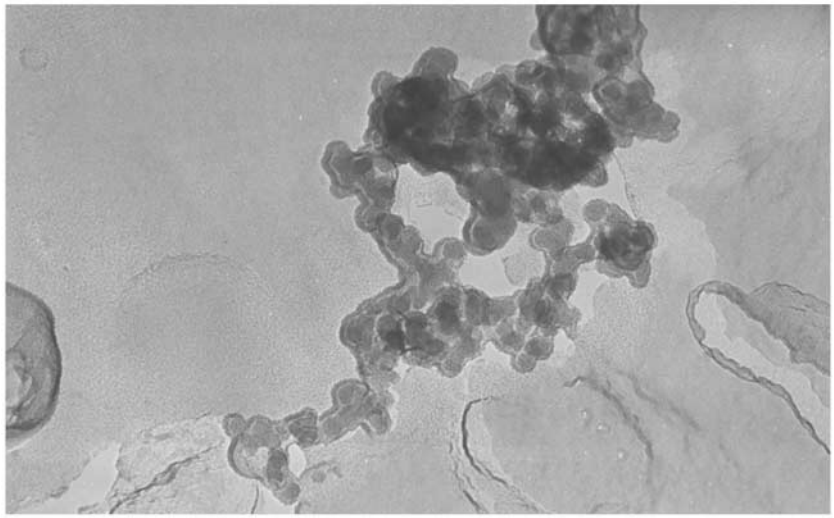

Figure 6. Transmission electron microscope observation of aggregated carbonaceous particles. These particles are made of a soot core imbedded in a non-absorbing coating.

mode 2 towards the end of the measurement period, that is to say when MD was at its highest. Since mineral aerosols are usually considered as non-hydrophilic, σ_n and d_n will be assumed to be independent of rh.

[26] The same method can be applied to the determination of the sea salt component, but one has to be aware that this time the mass and number characteristics of the mode retrieved by this method correspond to 'wet' conditions. Indeed, the ambient aerosol was not dried before entering the cascade impactor. By using a mean rh value measured on the sampling site, and an hygroscopic growth model [*Hänel*, 1976], it is possible to retrieve the dry sea salt characteristics. The uncertainties attached to this retrieval are mainly linked to the choice of a constant rh value that is not necessarily representative of the rh variations over the whole duration of the several hours long sampling. The number gmd and gsd of the dry sea salt population are found to be: $d_n = 0.45 \pm 0.10$ μm and $\sigma_n = 1.9 \pm 0.2$. These values are consistent with those indicated by *Hess et al.* [1998] for the dry sea salt accumulation mode ($d_n = 0.4$ μm; $\sigma_n = 2.0$). With an assumed mass density of 2.1 g/cm^3 [*Blanchard and Woodcock*, 1980] for sea salt, the number amplitudes of the sea salt accumulation mode can be computed for each impactor. The order of magnitude of their value is about one tenth of the amplitude of mode 2, but these results that integrate the time-variability over the sampling duration cannot be compared simply to the punctual determination of the amplitude of mode 2.

[27] Filter analysis by IC for particles collected at ambient humidity (rh ca 85%) by the EGA cascade impactor show the average size range of chloride, nitrate, and sulfate ions on the 5 stages and backup filter of the impactor (Figure 8). Chloride can be linked directly to sea salt, and nitrate mainly results from reactions of nitric acid with sodium chloride or aerosol crustal material [*Seinfeld and Pandis*, 1998]. Both of them are found in a coarse supermicron mode (CM) even though 14% of the nitrate mass is found on stage 3, that is to say in a smaller mode than the rest. As for sulfate, it is the only inorganic soluble species with a significant mass fraction in the submicron range. In order to achieve more precision in the fine size classes NSS has been determined by XRF for each stage of the DLPI. Deconvolution of these mass measurements show that, at ambient humidity, two NSS modes can be detected: a submicron mode (NSS1, with gmd = 0.43 μm, and gsd = 1.86) accounting for 60 % of the total sulfate mass, and a relatively coarse mode (NSS2, with gmd = 2.56 μm, and gsd = 1.70) accounting for the rest. Conversion of these mass parameters into number ones by the means of (5) and (6) yields respective gsd = 0.14 and 1.10 μm for the two modes in humid conditions. These values, along with the ones for dry conditions obtained by using *Hänel*'s [1976] model, are summarized in Table 4. The finest NSS containing particles, sulfates probably produced by gas phase conversion, are located in the same size range as CC1 particles, that is to say in mode 1 of the overall size distribution. By using NSS mass concentrations, taking into account that about 60% of NSS is in mode 1, the dry gmds

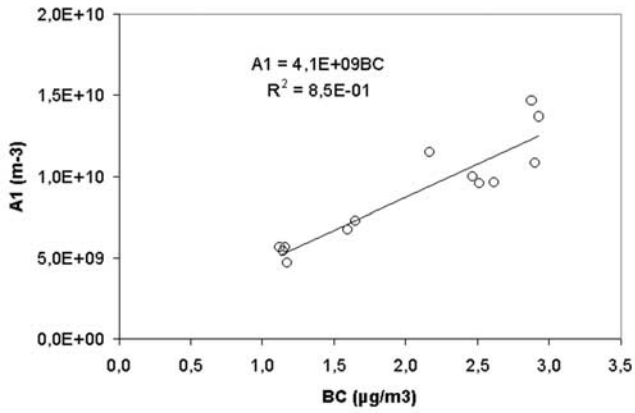

Figure 7. Correlation between the (number) amplitude of the finest aerosol mode and BC concentrations derived from aethalometer measurements. With $r^2 = 0.85$ and 13 measurements, this correlation is significant at the 99.9% confidence level.

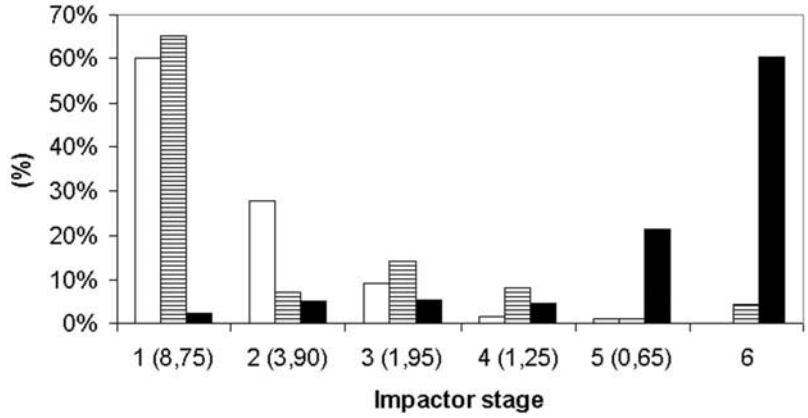

Figure 8. Average proportions determined by ion chromatography of chloride (white bars), nitrate (striped bars), and sulfate (black bars) ions collected on each stage of the cascade impactor. The 50% cut-off size of each stage is indicated in μm beside its number.

computed above, and the sulfate mass density (1.8 g/cm^3), it is possible to determine the number concentration of sulfate particles in the fine sulfate mode by:

$$N_{1,NSS} = 0.6C_{NSS}/\left(\pi/6.\rho_{NSS}.(gmd)^3\right), \quad (10)$$

and to compare it to the number amplitude of mode 1 when available. It is found that on average $N_{1,NSS} = 0.24A_1$, which approximately amounts to the 30 (non carbonaceous) percents that were still missing in mode 1. The same procedure applied to NSS2 shows that $N_{2,NSS} = 0.46A_2$, which does not explain all the 70% missing particles in mode 2, but shows that a significant fraction (at least 56%) of this mode is made of water-soluble particles (10% SS, and 46% sulfates). The missing component in mode 2 will be assumed to be made mostly of a nitrate (WS) population having the same distribution parameters as mode 2. Table 5 presents a summary of the number composition of modes 1 and 2.

4. Discussion

4.1. Origin of the Aerosol Carbonaceous Components at Goa

[28] Results detailed above show that in spite of their low contribution to the atmospheric mass load, soot particles constitute the major part of mode 1, and thus dominate the number size distribution of the aerosol in the submicron range. Particles in this size range are known to be the most optically active, at least in the visible spectrum. This explains why, regarding aerosol optical properties, carbonaceous aerosols have been shown to play a disproportionate part relatively to their mass contribution [*Satheesh et al.*, 1999; *Ramanathan et al.*, 2001]. The importance of this part is conditioned by their chemical and physical characteristics (apportionment between absorbing BC and scattering POM, state of mixing, size distribution, ...). These characteristics themselves depend on the particle origin (fossil fuel or biomass burning). Thus, it is important to assess the relative contributions of these two types of combustion to emissions. This is made possible by using the fact that K is a tracer of biomass burning. Indeed, fossil fuel combustion BC does not contain K. Moreover, the ratio of the biomass burning fraction of K (K_{BB}) to the corresponding BC (BC_{BB}) is fairly constant close to the sources, though it might later decrease during the aging process [*Cachier et al.*, 1991]. A typical value for this ratio at the source is 0.52 ± 0.11 [*Cachier et al.*, 1991; *Ferek et al.*, 1998]. This yields

$$BC_{BB} = 1.92\,K_{BB}, \quad (11)$$

in which K_{BB} can be determined from XRF analysis of the nuclepore samples by subtracting the sea-salt and mineral dust contributions to the overall atmospheric load in K. These contributions being respectively 1% and 1.36% of the SS and MD contents [*Seinfeld and Pandis*, 1998] one finally obtains:

$$BC_{BB} = 1.92\,K(1 - 0.01SS - 0.0136MD) \quad (12)$$

Table 4. Mass and Number Characteristics of the Two Particle Populations Into Which NSS Particles Can be Found[a]

	NSS1	NSS2
Mass %	60	40
rh, %	0/85	0/85
Mass gmd	0.25/0.43	1.50/2.56
Number gmd	0.08/0.14	0.64/1.10
σ	1.86	1.70

[a]The characteristics of NSS1 and NSS2 have been determined for ambient humidity (rh = 85%) by deconvolution of XRF analysis of low-pressure impactor stages. Values for dry conditions have been computed from *Hänel*'s [1976] hygroscopic model.

Table 5. Summary of the Geometric Number Mean Diameters and Geometric Standard Deviations of the Various Components of the Goa Aerosol[a]

		Mode 1		Mode 2				
	rh, %	CC1	NSS1	NSS2	BC2	SS	MD	WS
gmd, μm	0	0.08	0.08	0.64	0.40	0.45	1.50	0.40
Percent	85	0.08	0.14	1.10	0.40	0.77	1.50	0.69
gsd	-	1.8	1.86	1.7	1.7	1.9	1.6	1.7
Percent	-	70	24	46	10	10	10	24

[a]Here, gsd, geometric standard deviations. Geometric mean diameter (gmd) values are given for dry and wet (rh = 85%) conditions. The contributions (%) of each of these components to the amplitude of modes 1 and 2 are also reported (see text for details).

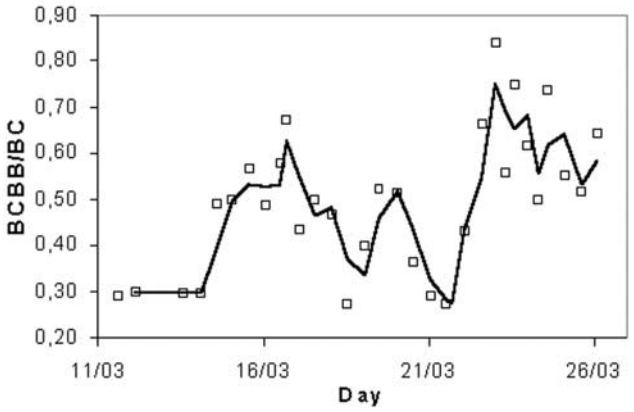

Figure 9. Variation with time of the fraction of black carbon (BC) produced by biomass burning (BCBB/BC). The rest results from fossil fuel combustion.

The BC_{BB}/BC ratio indicates the proportion of BC that can be attributed to biomass burning. It has to be noted that because the K_{BB}/BC_{BB} value adopted to derive (12) is the one valid close the source, using this equation and BC measurements provides a lower limit for BC_{BB}/BC. This ratio is found to vary greatly during the measurement period (Figure 9). Between March 11 and 14, around March 19, and March 22, BC_{BB}/BC is at its lowest and biomass burning then explains about 30% of the BC atmospheric loading. This is in good agreement with the proportion (21 ± 8%) obtained on March 10 or before by *Novakov et al.* [2000] in the same INDOEX area. Nonetheless, after March 10 three successive outbursts of biomass burning are observed (Figure 9). During the third one (around March 23), as much as 70% of the BC can be explained by this type of combustion. This is in good qualitative agreement with satellite observations reported by *Leon et al.* [2001] showing that the number of fires increased sharply in March over India. Indeed, it is a common agricultural practice in India to set cultivated land on fire before the first rains, and the frequency of fire events increases with time as one gets closer to the onset of the rainy season. The possible impact of this variability in carbonaceous particle sources on the aerosol optical properties is examined by S. C. Alfaro et al. (manuscript in preparation, 2003).

4.2. Interpretation of the Variability of TPM and PM1 Concentrations at Goa

[29] As already mentioned above a decrease in TPM and PM1 concentrations was observed at Goa during the first 12 days of March. This decrease can be explained by a change in meteorological conditions between February and March [*Leon et al.*, 2001]. In February the air masses arriving at Goa had a northeastern or eastern origin and had traveled a long way over the land and active pollution sources, whereas in early March the wind direction shifted to a northern position. In the latter case the air masses that followed the coast before reaching our measurement site had a smaller aerosol load. By early March, the biomass burning season had not yet started and, independent of the wind direction, the carbonaceous components mostly resulted from fossil fuel combustion as shown by *Novakov et al.*'s [2000] results and our own. After March 12, sporadic variations in PM1 can be attributed essentially to biomass burning outbursts. During this period, the PM1/TPM ratio remains approximately constant except between March 22 and 24 when a long range input of mineral dust originating from Pakistani deserts selectively increased the aerosol coarse fraction.

4.3. Comparison With Other INDOEX Results

4.3.1. Mass Concentrations

[30] Monthly and weekly averages of aerosol PM1 mass concentration and composition for KCO [*Chowdhury et al.*, 2001; *Lelieveld et al.*, 2001] are the only ones available in the literature for comparison with our results. Unfortunately, these measurements limited to the 'fine aerosol component' were performed in February 1999. Thus, they do not overlap with ours that were mostly performed in March and were not restricted to the fine particle range, except in the case of BC for which aethalometer measurements are available from February 16 at Goa. At this site, the average BC concentration for the second half of February is 4,02 ± 0.46 $\mu g/m^3$, a value substantially larger than the one (2.38 $\mu g/m^3$) measured at KCO, but still of the same order of magnitude. This similarity in concentrations between Goa and KCO is also observed for sulfate (3.6 ± 1.6 at Goa by the end of March, and 6.3 at KCO in February). Moreover, the BC/PM1 mass fraction measured at KCO (6–11%) by *Chowdhury et al.* [2001] is the same as at Goa (10%). This confirms that in spite of a spatial concentration gradient already observed downwind of the Indian subcontinent [e.g., *Jayaraman et al.*, 1998; *Satheesh et al.*, 1998], the winter monsoon is very efficient at transporting the pollution haze over long distances, and that during this transport intensive aerosol characteristics such as the BC/PM1 ratio remain practically unchanged.

4.3.2. Size Distribution

[31] Results above show that aerosol number size distributions at Goa can be modeled by using three lognormally distributed populations. The amplitude of the finest mode being strongly correlated to BC, concentrations of this component can be used to estimate A1 from (9). Thus, a BC average of 2.18 ± 1.01 $\mu g/m^3$ for March 1999 yields a value of A1 between 4.80 10^9 and 1.30 10^{10} m^{-3}. Except during long-range transport of dust when A1/A2 is only 500, the amplitude of mode 2 is about 1300 times smaller than A1. For lack of sufficient precision A3 is considered as constant (=4.0 $10^5/m^3$), even though adoption of this value determined from measurements essentially performed during the dust peak probably leads to an overestimation of the coarse mode in usual conditions. The lower and upper limits of the number size distribution determined for March 1999 at Goa are plotted in Figure 10. Except for sizes larger than 3.5 μm for which the predicted overestimation is clearly observed, the previous limits encompass measurements performed over the Arabian Sea during the pre-INDOEX campaigns [*Jayaraman et al.*, 1998; *Satheesh et al.*, 1998]. Nonetheless, with the BC values observed at Goa in March, the high amplitude of mode 1 found by Jayaraman et al. for 'coastal India' cannot be explained. It would take BC concentrations as large as 12 $\mu g/m^3$ to retrieve these values. This concentration, three times larger than the maximum reached at Goa by the end of February, can possibly be

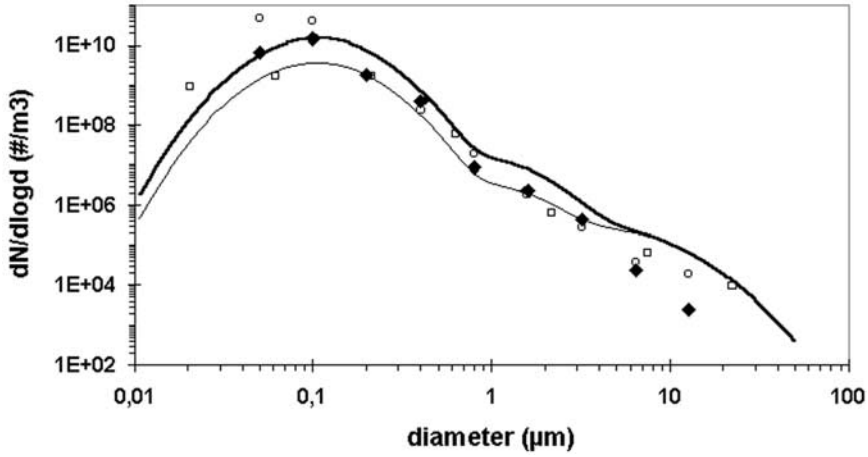

Figure 10. Lower (thin line) an upper (thick line) limits of the aerosol number size distribution measured in March at Goa are compared to measurements made in 'Coastal India' (open circles), the 'Arabian Sea' (solid diamonds) by *Jarayaman et al.* [1998], and in the Maldives (open squares) by *Satheesh et al.* [1999].

obtained in the vicinity of large cities such as Mumbaï, but there is a lack of published data to support this assumption.

[32] It can also be noted that the lower limit of Goa values for March compares well to KCO measurements. This indicates that the local variability of number size distributions at the coastal site can be of the same order of magnitude as the concentration reduction resulting from transport of the pollution cloud between the continent and the Maldives. In other words, it is not straightforward when comparing concentrations at a particular site and upwind of it, to assess the relative parts played by transport and concentration variability at the source in the observed concentration gradient.

5. Summary and Conclusion

[33] During March 1999 TPM concentrations at ground level varied between 27 and 120 $\mu g/m^3$ at the coastal site of Goa. This important mass variability mostly results from changes in meteorological conditions. Indeed, input to the measurement site of coarse mineral particles from faraway sources became possible during the second half of the month. A lower variability was observed for PM1 concentrations. In this size range, carbonaceous components largely dominate the number size distribution. From a situation where they mostly originate from fossil fuel combustion at the beginning of the month, the contribution of biomass burning is found to increase, though not regularly, in keeping with the number of fires observed from satellites on the Indian sub-continent. This has consequences on the PM1 composition. In particular, the relative importance of organic components is found to vary during the observation period. Because POM is mainly found under the form of soot core coatings, and because it is much less absorbing and considered as more hydrophilic than BC, this could significantly affect the aerosol optical properties. The correlation between relative humidity, composition and scattering properties is the object of a future study (S. C. Alfaro et al., manuscript in preparation, 2003).

[34] Comparison of our results for March 1999 with measurements performed at different times and locations over the northern Indian Ocean shows that differences observed between sites are generally not larger than the variability of aerosol characteristics (size distribution, composition) at Goa. This emphasizes the ability of the winter monsoon to homogenize aerosol properties. It also indicates that aerosol models deduced from observations made at a single site can probably be considered as representative of large INDOEX areas provided they integrate the time variability of the aerosol characteristics at the measurement site.

[35] **Acknowledgments.** This work was supported by the Programme National de Chimie Atmosphérique in the framework of the 'Aérosols-Climat' project. The authors would like to thank F. Aulagnier and R. Sarda for analyzing carbon filters. They are also grateful to P. Sarode and G. M. Naik for hosting the instruments on the terrace of the Instrumentation Centre of Goa University.

References

Bergametti, G., R. Vie le Sage, B. Grubis, B. Dulieu, and C. Elichegaray, Relation between particle concentration in the atmosphere and aerosol collection efficiency, *Environ. Technol. Lett.*, *3*, 297–304, 1982.

Blanchard, C. D., and H. A. Woodcock, The production, concentration, and vertical distribution of the sea-salt aerosol, *Ann. N. Y. Acad. Sci.*, *338*, 330–347, 1980.

Cachier, H., M. P. Brémond, and P. Buat-Ménard, Determination of atmospheric soot carbon with a simple thermal method, *Tellus, Ser. B*, *41*, 379–390, 1989.

Cachier, H., J. Ducret, M. P. Brémond, V. Youbué, J. P. Lacaux, A. Gaudichet, and J. Baudet, Biomass burning aerosols in a savanna region of the Ivory Coast, in *Global Biomass Burning*, edited by J. S. Levine, pp. 174–180, MIT Press, Cambridge, Mass., 1991.

Chiapello, I., G. Bergametti, B. Chatenet, F. Dulac, I. Jankowiak, C. Liousse, and E. S. Soares, Contribution of the different aerosol species to the aerosol mass load and optical depth over the northeastern tropical Atlantic, *J. Geophys. Res.*, *104*(D4), 4025–4036, 1999.

Chowdhury, Z., L. S. Hughes, L. G. Salmon, and G. R. Cass, Atmospheric particle size and composition measurements to support light extinction calculations over the Indian Ocean, *J. Geophys. Res.*, *106*(D22), 28,597–28,605, 2001.

Ferek, R. J., J. S. Reid, P. V. Hobbs, D. R. Blake, and C. Liousse, Emission factors of hydrocarbons, halocarbons, trace gases and particles from biomass burning in Brazil, *J. Geophys. Res.*, *103*(D24), 32,107–32,118, 1998.

Gaudichet, A., F. Echalar, B. Chatenet, J. P. Quisefit, and G. Malingre, Trace elements in tropical African savanna biomass burning aerosols, *J. Atmos. Chem.*, *22*, 19–39, 1995.

Goldschmidt, V. M., *Geochemistry*, *Int. Ser. Monogr. Phys.*, Muir ed., 2nd ed., Oxford Univ. Press, New York, 1958.

Gomes, L., G. Bergametti, F. Dulac, and U. Ezat, Assessing the actual size distribution of atmospheric aerosols collected with a cascade impactor, *J. Aerosol. Sci.*, *21*, 47–59, 1990.

Guazzotti, S. A., K. R. Coffee, and K. A. Prather, Continuous measurements of size resolved particle chemistry during INDOEX-Intensive Field Phase 99, *J. Geophys. Res.*, *106*(D22), 28,607–28,627, 2001.

Hänel, G., The properties of atmospheric aerosol particles as functions of the relative humidity and thermodynamic equilibrium with surrounding moist air, *Adv. Geophys.*, *19*, 73–188, 1976.

Hess, M., P. Koepke, and I. Schult, Optical properties of aerosols and clouds: The software package OPAC, *Bull. Am. Meteorol. Soc.*, *79*, 831–844, 1998.

Hopke, P. K., Y. Xie, T. Raunemaa, S. Biegalski, S. Lansberger, W. Maenhaut, P. Artaxo, and D. Cohen, Characterization of the gent stacked filter unit PM10 sampler, *Aerosol Sci. Technol.*, *27*(6), 726–735, 1997.

Jayaraman, A., D. Lubin, S. Ramachandran, V. Ramanathan, E. Woodbridge, W. D. Collins, and Z. S. Zalpuri, Direct observations of aerosol radiative forcing over the tropical Indian Ocean during the January–February 1996 pre-INDOEX cruise, *J. Geophys. Res.*, *103*(D12), 13,827–13,836, 1998.

Lelieveld, J., et al., The Indian Ocean Experiment: Widespread air pollution from South and Southeast Asia, *Science*, *291*, 1031–1036, 2001.

Leon, J. F., et al., Large scale advection of continental aerosols during INDOEX, *J. Geophys. Res.*, *106*(D22), 28,427–28,439, 2001.

Liousse, C., J. E. Penner, C. Chang, J. J. Walton, H. Eddleman, and H. Cachier, A global three-dimensional model study of carbonaceous aerosols, *J. Geophys. Res.*, *101*(D14), 19,411–19,432, 1996.

Liu, B. Y., and D. Y. Piu, Aerosol sampling inlets and inhalable particles, *Atmos. Environ.*, *15*, 589–600, 1980.

Martins, J. V., P. Artaxo, C. Liousse, J. S. Reid, P. V. Hobbs, and Y. J. Kaufman, Effects of black carbon content, particle size, and mixing on light absorption by aerosols from biomass burning in Brazil, *J. Geophys. Res.*, *103*(D24), 32,041–32,050, 1998.

Novakov, T., M. O. Andreae, R. Gabriel, T. W. Kirchstetter, O. L. Mayol-Bracero, and V. Ramanathan, Origin of carbonaceous aerosols over the tropical Indian Ocean: Biomass burning or fossil fuels?, *Geophys. Res. Lett.*, *27*, 4061–4064, 2000.

Peterschmitt, E., Les couvertures ferralitiques des Ghats Occidentaux (Inde du Sud): Caractères généraux sur l'escarpement et dégradation par hydromorphie sur le revers, Ph.D. thesis 145 pp., Trav. Sect. Sci. Technol. de l'Inst. Français de Pondichery, Univ. de Nancy I, Nancy, France, 1993.

Ramanathan, V., et al., Indian Ocean Experiment (INDOEX) White Paper, *C*^{4} *Publ. 143*, Scripps Inst. of Oceanogr., Univ. of Calif., San Diego, La Jolla, 1995.

Ramanathan, V., et al., Indian Ocean Experiment: An integrated analysis of the climate forcing and effects of the great Indo-Asian hase, *J. Geophys. Res.*, *106*(D22), 28,371–28,398, 2001.

Reid, J. S., and P. V. Hobbs, Physical and optical properties of young smoke from individual biomass fires in Brazil, *J. Geophys. Res.*, *103*(D4), 32,013–32,030, 1998.

Satheesh, S. K., K. K. Moorthy, and B. V. K. Murthy, Spatial gradients in aerosol characteristics over the Arabian sea and Indian Ocean, *J. Geophys. Res.*, *103*(D20), 26,183–26,192, 1998.

Satheesh, S. K., V. Ramanathan, X. Li-Jones, J. M. Lobert, I. A. Podgorny, J. M. Prospero, B. N. Holben, and N. G. Loeb, A model for the natural and anthropogenic aerosols over the tropical Indian Ocean derived from Indian Ocean Experiment data, *J. Geophys. Res.*, *104*(D22), 27,421–27,440, 1999.

Saxena, P., L. Hildemann, P. H. McMurry, and J. H. Seinfeld, Organics alter hygroscopic behavior of atmospheric particles, *J. Geophys. Res.*, *100*(D9), 18,755–18,770, 1995.

Seinfeld, J. H., and S. N. Pandis, *Atmospheric Chemistry and Physics: From Air Pollution to Climate Change*, 1326 pp., John Wiley, New York, 1998.

Taylor, S. R., Abundance of chemical elements in the continental crust: A new table, *Geochim. Cosmochim. Acta*, *28*, 1273–1285, 1964.

S. C. Alfaro, A. Gaudichet, L. Gomes, M. Maillé, and J. L. Rajot, UMR-CNRS 7583, Université PVII/PXII, 61, avenue du général de Gaulle, 94010 Créteil, France. (alfaro@lisa.univ-paris12.fr)

H. Cachier, LSCE, CEA-CNRS 1572, L'orme des merisiers 709, 91191 Gif/Yvette Cedex, France.